

**High nitrite accumulation in hydrogenotrophic denitrification at low temperature
Transcriptional regulation and microbial community succession**

Zhou, Jianmin; Ding, Lei; Cui, Changzheng; Lindeboom, Ralph E.F.

DOI

[10.1016/j.watres.2024.122144](https://doi.org/10.1016/j.watres.2024.122144)

Publication date

2024

Document Version

Final published version

Published in

Water Research

Citation (APA)

Zhou, J., Ding, L., Cui, C., & Lindeboom, R. E. F. (2024). High nitrite accumulation in hydrogenotrophic denitrification at low temperature: Transcriptional regulation and microbial community succession. *Water Research*, 263, Article 122144. <https://doi.org/10.1016/j.watres.2024.122144>

Important note

To cite this publication, please use the final published version (if applicable).
Please check the document version above.

Copyright

Other than for strictly personal use, it is not permitted to download, forward or distribute the text or part of it, without the consent of the author(s) and/or copyright holder(s), unless the work is under an open content license such as Creative Commons.

Takedown policy

Please contact us and provide details if you believe this document breaches copyrights.
We will remove access to the work immediately and investigate your claim.



High nitrite accumulation in hydrogenotrophic denitrification at low temperature: Transcriptional regulation and microbial community succession

Jianmin Zhou^a, Lei Ding^{a,*}, Changzheng Cui^a, Ralph E.F. Lindeboom^{b,*}

^a National Engineering Research Center of Industrial Wastewater Detoxication and Resource Recovery, School of Resources and Environmental Engineering, East China University of Science and Technology, Shanghai 200237, China

^b Sanitary Engineering Section, Department of Water Management, Delft University of Technology, Delft 2628 CN, the Netherlands

ARTICLE INFO

Keywords:

Hydrogenotrophic denitrification
Low temperature
Nitrite accumulation
Denitrifying gene expression
Paracoccus
Hydrogenophaga

ABSTRACT

High Pressure Hydrogenotrophic Denitrification (HPHD) provided a promising alternative for efficient and clean nitrate removal. In particular, the denitrification rates at low temperature could be compensated by elevated H₂ partial pressure. However, nitrite reduction was strongly inhibited while nitrate reduction was barely affected at low temperature. In this study, the nitrate reduction gradually recovered under long-term low temperature stress, while nitrite accumulation increased from 0.1 to 41.0 mg N/L. The activities of the electron transport system (ETS), nitrate reductase (NAR), and nitrite reductase (NIR) decreased by 45.8 %, 27.3 %, and 39.3 %, respectively, as the temperature dropped from 30 °C to 15 °C. Real time quantitative PCR analysis revealed that the denitrifying gene expression rather than gene abundance regulated nitrogen biotransformation. The substantial nitrite accumulation was attributed to the significant up-regulation by 54.7 % of *narG* gene expression and down-regulation by 73.7 % of *nirS* gene expression in hydrogenotrophic denitrifiers. In addition, the *nirS*-gene-bearing denitrifiers were more sensitive to low temperature compared to those bearing *nirK* gene. The dominant populations shifted from the genera *Paracoccus* to *Hydrogenophaga* under long-term low temperature stress. Overall, this study revealed the microbial mechanism of high nitrite accumulation in hydrogenotrophic denitrification at low temperature.

1. Introduction

Over the past century, human activities have exerted an enormous impact on the global nitrogen cycle while causing unacceptable nitrate contamination of water resources, and it was mainly attributed to fossil fuel combustion and the application of nitrogen-based fertilizers in intensive agriculture (Canfield et al., 2010; Kuypers et al., 2018). As a critical anaerobic process in the nitrogen cycle, bio-denitrification is also the major pathway to remove nitrate from wastewater. In heterotrophic denitrification, organics working as electron donors are indispensable for denitrifiers to reduce oxidized nitrogen species. Exogenous organic carbon is often required in the nitrogen polishing unit of the conventional wastewater treatment facility due to the excessive control of upstream organic pollutants (Ren and Pagilla, 2022; Tian and Yu, 2020). However, it is undoubtedly counterproductive to the concept of water sector upgrading that focuses on energy and resource recovery and

carbon footprint reduction (Ren and Pagilla, 2022). Autotrophic denitrification thus has been suggested for treating wastewater with a low C/N ratio, in which hydrogenotrophic configurations elicited much interest due to its clean nature, especially in the oligotrophic groundwater and drinking water or tertiary nitrogen removal (Karanasios et al., 2010; Lee and Rittmann, 2002; Li et al., 2013; Tang et al., 2011).

Hydrogenotrophic denitrification capturing CO₂ for biosynthesis is an excellent alternative to facilitate carbon neutrality or negative emissions in wastewater treatment plants. The strategies of implementing hydrogenotrophic denitrification and their advantages were discussed comprehensively in previous studies (Albina et al., 2019; Karanasios et al., 2010; Rittmann, 2018), and considerable effort has been made to improve H₂ utilization and system security (Epszstein et al., 2017; Lee and Rittmann, 2002; Rezanian et al., 2007). However, the low solubility of H₂ gas under atmospheric pressure with poor gas-liquid mass transfer is the primary roadblock for full-scale engineering

* Corresponding authors.

E-mail addresses: leiding@ecust.edu.cn (L. Ding), R.E.F.Lindeboom@tudelft.nl (R.E.F. Lindeboom).

<https://doi.org/10.1016/j.watres.2024.122144>

Received 18 April 2024; Received in revised form 12 July 2024; Accepted 23 July 2024

Available online 25 July 2024

0043-1354/© 2024 Elsevier Ltd. All rights reserved, including those for text and data mining, AI training, and similar technologies.

applications. Given the circumstances, high-rate hydrogenotrophic denitrification based on pressurization systems was successfully reported (Epsztein et al., 2016, 2017; Keisar et al., 2021; Zhou et al., 2022), and High Pressure Hydrogenotrophic Denitrification (HPHD) provided a promising approach for sustaining effective low temperature denitrification (Zhou et al., 2022).

Temperature is a crucial factor that directly affects the efficiency of biological denitrification. Although denitrifying activity was observed over a wide temperature range, the performance of both heterotrophic and autotrophic denitrification deteriorated at psychrophilic temperatures (Di Capua et al., 2017; Shen et al., 2020), which was a dilemma for biological nitrogen removal processes operating under cold conditions. In our previous study, the denitrification rate and efficiency of HPHD at low temperature could be maintained by increasing H_2 partial pressure. However, transient nitrite accumulation during denitrification was inevitable. The dramatic inhibition of nitrite reduction was observed, whereas the nitrate reduction was unexpectedly almost unaffected (Zhou et al., 2022). It would take much more denitrification time and costs for complete nitrogen removal when treating cold nitrate-contaminated waters. Thus, a better understanding of high nitrite accumulation at low temperatures is of great necessity to improve cost-effective performance.

The reduction of NO_3^- to N_2 in denitrification process is inseparable from the participation of electrons generated by the oxidation of substrates. For hydrogenotrophic denitrifiers, the hydrogenase responsible for H_2 oxidation feeds the electrons directly into the respiratory chain (Bowien and Schlegel, 1981; Knowles, 1980). The electrons are ultimately consumed by denitrifying enzymes after being transferred via the electron transport system (ETS) containing quinone pool and various electron carrier proteins. Thus, any restriction on the electron transport and consumption would affect the final denitrification rate. The ETS and denitrifying enzyme activities have been used to assess the effects of environmental contaminants on heterotrophic denitrification, such as antibiotics (Chen et al., 2021), pesticides (Su et al., 2019) and CO_2 (Wan et al., 2016). Meanwhile, their dynamics are regulated by temperature. In addition, low temperature shock would negatively affect the expression of denitrifying functional genes, leading to the accumulation of denitrification intermediates and a sharp decrease in the denitrification rate (Saleh-Lakha et al., 2009; Wang et al., 2018). The denitrifying functional gene abundance, as well as microbial community structure, might be altered when the system suffered from long-term low temperature stress (Chen et al., 2017; Liao et al., 2018). However, the relevance between these factors and the varied responses of different denitrification steps to low temperature conditions is currently unclear.

In this study, the effects of long-term low temperature on HPHD were investigated. Firstly, the continuous operation in a cyclic mode was conducted as a sequencing batch reactor (SBR) to evaluate the deterioration of HPHD at low temperature. Then, the electron transport and consumption during hydrogenotrophic denitrification under different temperatures were analyzed by comparing ETS, NAR, and NIR activities. Moreover, the expression and abundance variation of denitrifying functional genes (*narG*, *nirS*, *nirK*, and *nosZ*) in response to low temperature stress were investigated. Finally, the succession of the microbial community was monitored through high-throughput sequencing targeting the 16S rRNA gene. This work was undertaken to reveal the microbial mechanism of high nitrite accumulation in hydrogenotrophic denitrification, which might be beneficial to seek suitable strategies to eliminate nitrite accumulation in NO_3^- remediation or to offer a potential alternative for the emerging partial-denitrification process (Shinoda et al., 2020).

2. Materials and methods

2.1. Bioreactor setup

The experiments were conducted in a stainless-steel pressurized

reactor (Fig. S1) with an effective volume of 0.65 L. A detailed description of the reactor was given in a previous publication (Zhou et al., 2022). The inoculated sludge was derived from a hydrogenotrophic denitrification reactor that had been operating for more than three months (Zhou et al., 2022), and the mixed liquid volatile suspended solids (MLVSS) were maintained at 0.5 g/L by decanting biomass regularly. Ultrapure water enriched with 0.722 g/L KNO_3 , 2 g/L $NaHCO_3$, and several other necessary nutrients was fed as synthetic wastewater for all experiments (Zhou et al., 2022). The pH was controlled within the optimal range of 7.6–8.6 by phosphate buffer (Karanasios et al., 2010). An agitation rate of 200 rpm was controlled by magnetic stirring to ensure the mixture was fully homogeneous.

2.2. Description of experiments

Continuous operation of HPHD system was conducted in a cycling mode as SBR at 30 °C and 15 °C, respectively. The reactor worked with three 8 h cycles per day, and each cycle consisted of 20 min feeding, 5 h stirring, 2.5 h settling, and 10 min decanting. In feeding time, synthetic wastewater was added to make the initial working volume to be 0.5 L, and the denitrifying medium was purged with H_2 to expel the air in the headspace in each cycle. The denitrification process was conducted under a constant H_2 partial pressure of 4 bars (absolute pressure). Influent and effluent samples of mixed liquor were collected at the end of the stirring period for NO_3^- -N and NO_2^- -N determination (batches run at night were not sampled, and the results for each day were the average of the other two batches). In addition, the sludge was also collected after long-term incubation by centrifugation (10,000 rpm, 10 min at 4 °C) plus washing with 0.01 M PBS buffer (pH = 7.4) and stored in -80 °C for subsequent analysis of microflora.

Batch experiments were also conducted at the end of each phase to investigate the effects of cooling on denitrifying activity. Each batch experiment was run for 5 h, and the environmental conditions were constant with the mentioned above, including hydrogen pressure and temperature. The NO_3^- -N and NO_2^- -N concentrations were detected hourly. The sludge samples were collected at 3 h of each batch to analyze denitrifying enzyme activity, ETS activity, denitrifying gene expression, and abundance.

2.3. ETS and denitrifying enzyme activities assay

The denitrifier suspensions were prepared for the determination of ETS, NAR, and NIR activities. 10 mL of mixture samples collected from batch experiments were centrifuged at 4000 rpm for 10 min, rinsed thrice with 0.01 M PBS buffer (pH = 7.4), and then resuspended for spare. The NAR and NIR activities were determined using commercial assay kits (Solarbio, China). Briefly, the resuspended bacteria were sonicated for 3 min and centrifuged at 10,000 rpm and 4 °C for 10 min to obtain the crude extracts. The crude extract and electron donor were first injected into anaerobic cuvettes fitted with rubber stoppers, followed by nitrate or nitrite to initiate the reaction. The production or consumption of nitrite was analyzed at different time intervals.

The measurement of ETS activity was based on the rate of 2-(p-iodophenyl)-3-(p-nitrophenyl)-5-phenyl-tetrazolium chloride (INT) reduced to red-coloured INT-formazan (Broberg, 1985). 1 mL of suspension was mixed with 9 mL homogenization buffer, and the cells in the mixture were disrupted by ultrasonication in an ice-water bath for 3 min. The cell-free homogenates were harvested by centrifugation at 10,000 rpm in a refrigerated centrifuge at 4 °C for 10 min. Then, 1 mL of cell-free extract was incubated with 1 mL substrate solution (1.25 mM NADH) and 0.5 mL INT solution (0.5 %) for 30 min. The reaction was terminated by adding 1 mL of the reaction termination solution. The absorbance of the INT-formazan formed was determined spectrophotometrically at 490 nm against blank as reference. Buffers and solutions in the assay are provided in Supplementary Materials. The protein content in cell-free extract was determined by the BCA protein assay kit (Sangon

Biotech, China).

2.4. Real-time quantitative PCR assay

In batch experiments, samples were collected after 3 h of feeding from the control (T30, 30 °C) and T15 (15 °C) treatment, at which the denitrification process was still in progress. The copy numbers and transcript levels of denitrifying functional gene (*narG*, *nirS*, *nirK*, and *nosZ*) were quantified by real-time quantitative PCR. The PCR procedure was performed on a MA-6000 real-time PCR detection system (Molarray, China), and information of the primers was listed in Table S1. The DNA and RNA were extracted from denitrifying sludge using Soil DNA/RNA kit (Omega, USA) following the manufacturer protocol, and the concentrations were determined by the NanoDrop spectrophotometer (NanoDrop 2000, Thermo Fisher Scientific, USA).

For qPCR assay, a 20 μ L real-time PCR mixture contained 10 μ L of 2 \times SYBR qPCR Master Mix (Vazyme, China), 0.4 μ L of forward and reverse specific primer (10 μ M), 1 μ L of DNA template, and 8.2 μ L of ddH₂O. The plasmids containing the denitrifying gene sequence from the extracted genomic DNA were prepared as standards, and the copy numbers were calculated from the concentration and size of the plasmids. Standard curves were generated using three replicates of 10-fold serial dilutions of plasmids as a template. The amplification efficiency of functional genes was 92.35 % - 98.44 % with R² values of 0.994 - 0.997 for calibration curves (Table S2). For RT-qPCR assay, the qualified and quantified total RNA was reverse-transcribed into cDNA by PrimeScript™ 1st stand cDNA Synthesis kit (Takara, Japan). Then, the cDNA was used as template for relative quantitative PCR analysis and 16S rRNA was used as a control for normalization between samples. The relative expression ratios of target genes were calculated using the 2^{- $\Delta\Delta$ CT} method (Livak and Schmittgen, 2001). The amplifications were performed at 95 °C for 5 min, followed by 40 cycles at 95 °C for 15 s and at 60 °C for 30 s. All the real-time quantitative PCR assays were performed in triplicate for each sample.

2.5. Microbial community analysis

Samples of denitrifying sludge were collected on Day 30 (30 °C) and Day 60 (15 °C) for the genomic DNA extraction of hydrogenotrophic denitrifiers to assess bacteria diversity and abundance. The V3-V4 hypervariable regions of the bacterial 16S rRNA genes were amplified with the primers 338F (5'-ACTCTACGGGAGGCAGCA-3') and 806R (5'-GGACTACHVGGGTWTCTAAT-3'). Sequencing was performed on the purified products using an Illumina MiSeq PE250 platform. The sequence analysis was processed with QIIME 2 (Bolyen et al., 2018), and taxonomy was assigned to amplicon sequence variants (ASVs) with the SILVA database (release 132). The details of DNA extraction, PCR amplification, and sequence analysis are available in Supplementary Materials.

2.6. Other analytical methods

The influent and effluent samples were collected using disposable syringes for the analyses of NO₃-N, NO₂-N after filtering through a disposable Waterman filter unit (0.22 μ m pore size). The MLVSS, NO₃-N, and NO₂-N were determined according to the standard methods (APHA, 2005). The pH and temperature were monitored online in real time by an embedded electrode sensor (InPro4550VP pH Probe, Switzerland). All the tests were conducted in triplicate and the results were expressed as mean \pm standard deviation. Significant differences between individual treatments were analyzed using independent samples *t*-test (SPSS statistics 26.0, IBM, USA), and *p* < 0.05 was considered to be statistically significant.

3. Results and discussion

3.1. Effects of temperature on denitrification performance in HPHD

The denitrification performance of HPHD system operating at the H₂ partial pressure of 4 bars under different temperatures was presented in Fig. 1. During phase I (Day 1–30), the temperature was set at 30 °C, the effluent NO₃-N and NO₂-N stabilized at low concentrations. The effluent NO₃-N was 2.9 \pm 2.0 mg/L on average, and effluent NO₂-N was below 1.0 mg/L except for the first two days (2.1 and 1.1 mg/L). The specific denitrification rate (SDR) ranged from 36.2 to 41.4 mg N/(gVSS-h) over phase I.

With the drop of temperature to 15 °C on Day 31, a steep increase to 45.6 mg/L in effluent NO₃-N was observed, while effluent NO₂-N was about 0.04 mg/L. This result suggested that nitrate reduction was immediately inhibited by low temperature shock, which was consistent with previous reports (Li et al., 2013). Subsequently, effluent NO₃-N gradually decreased until it recovered to a similar level in phase I by Day 48. The effluent NO₂-N still remained at an extremely low level during this period. Finally, stable NO₃-N removal was achieved, and the NO₂-N accumulation also emerged after a two-day rising transition period. The effluent NO₂-N accumulated from 0.1 to 41.0 mg N/L and maintained at 40.3 \pm 3.0 mg/L from Day 48 to Day 60. In addition, the SDR remained relatively stable (standard deviation less than 10 %) despite the effluent NO₃-N, NO₂-N varied during phase II. The SDR averaged 24.4 \pm 2.3 mg N/(gVSS-h) at 15 °C, which was about 58.9 % ~ 67.4 % of that of 30 °C.

It could be concluded that the NO₃-N reduction activity of the hydrogenotrophic denitrifying culture gradually recovered after 18 days of cold acclimation, and NO₃-N removal efficiency was more than 98.7 % under long-term low temperature stress. However, NO₂-N reduction rate at 15 °C was consistently much lower than that at 30 °C, and substantial and steady NO₂-N accumulated after Day 48, indicating that NO₂-N reduction was inhibited dramatically by low temperature.

The effects of low temperature on nitrate reduction and nitrite accumulation were further investigated by tracking the time courses of denitrification at 15 °C and 30 °C in a typical SBR cycle. As shown in Fig. 2a, the NO₃-N concentration declined linearly until exhaustion, and negligible NO₂-N was detected, with a maximum accumulation ratio of only 0.25 % at 30 °C. However, after long-term exposure to low temperature, NO₂-N concentration gradually increased until NO₃-N was almost depleted and peaked at 64.3 \pm 1.3 mg/L (Fig. 2b). The corresponding NO₂-N accumulation ratio remained at approximately 70 %. Interestingly, the nitrate reduction rate at 15 °C was even higher than

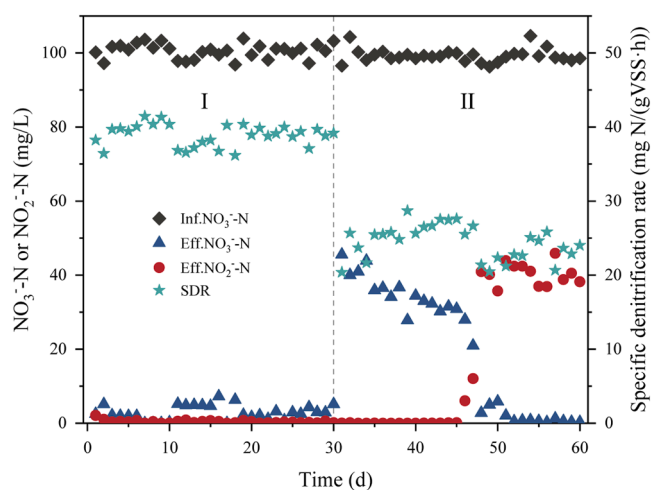


Fig. 1. Denitrification performance of HPHD system: NO₃-N, NO₂-N in the influent and effluent, and specific denitrification rate (SDR) under different temperatures. Phase I, Day 1–30 (30 °C), phase II, Day 31–60 (15 °C).

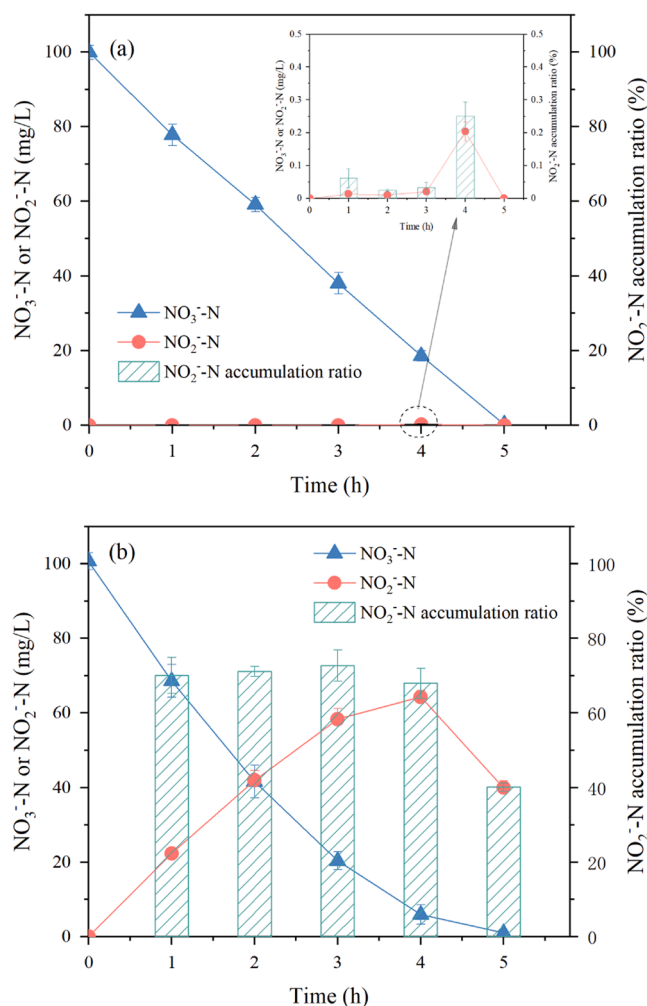


Fig. 2. NO₃-N, NO₂-N profiles and NO₂-N accumulation ratio in a typical SBR cycle at 30 °C (a) and 15 °C (b). Error bars represent standard deviations of three replicates.

that at 30 °C when nitrate was sufficient (0–3 h). These results suggested that the two denitrification steps were not synchronized effectively under low temperature conditions. It has been reported that competitive inhibition of nitrite by nitrate in heterotrophic denitrification led to a preferential nitrate reduction (Almeida et al., 1995). Our previous study confirmed that competitive inhibition was not caused by H₂ deficiency in HPHD (Zhou et al., 2022). Overall, the performance deterioration of hydrogenotrophic denitrification under long-term low temperature stress was mainly attributed to the strong inhibition of nitrite reduction and was independent of nitrate reduction. In addition, although it is possible to ensure effluent quality by extending hydraulic retention time, reducing nitrate loading rate (Wang et al., 2022), and increasing H₂ partial pressure (Zhou et al., 2022), these are compromises that sacrifice efficiency or increase inputs.

3.2. ETS and denitrifying enzyme activities in response to low temperature

In hydrogenotrophic denitrifiers, hydrogenase oxidizes H₂ to generate two electrons and introduces electrons into ETS (Knowles, 1980). Electrons are transferred by various electron carriers, such as ubiquinone and cytochrome c, and finally accepted by electron acceptors (Zumft, 1997). The NO₃⁻ is sequentially reduced to NO₂⁻, NO, N₂O and N₂, which are catalyzed by four denitrifying enzymes (NAR, NIR, NOR and NOS) (Fig. 3a). The relative activity of enzymes might sometimes be affected by denitrifier composition, but environmental factors

are the determinants (Wallenstein et al., 2006). As shown in Fig. 3b, compared with the control (T30), the ETS, NAR, and NIR activities in T15 treatment were significantly decreased by 45.8 %, 27.3 %, and 39.3 %, respectively ($p < 0.05$). This result showed that electron transport and consumption were inhibited under low temperature, which was consistent with the SDR decrease in phase II. When the temperature dropped from 30 °C to 15 °C, the decrease in ETS activity resulted in fewer electrons being transferred to NO₃⁻ and NO₂⁻. The electron consumption rates of NAR, NIR on Day 31 were 1.46 mmol e⁻/h and 0.73 mmol e⁻/h, respectively, which were only approximately 0.5 times those on Day 30 (Fig. 3c). Obviously, the inhibition of ETS and denitrifying enzyme activities of denitrifiers was directly responsible for the decline in the effluent quality of hydrogenotrophic denitrification process at low temperature.

It is worth noting that significant differences in electron consumption rate occurred at different incubation times under low temperature. Specifically, the electron consumption rate of NAR after 30 days of incubation (Day 60) at 15 °C was much higher than that on the first day (Day 31), suggesting that other factors, rather than the restoration of enzyme activity, promoted nitrate reduction. Furthermore, the total electron consumption rate increased from 2.19 mmol e⁻/h on Day 31 to 3.67 mmol e⁻/h on Day 60, implying that only partial NO₃-N conversion to gaseous products for temperature shock was not due to the limitation of available electrons. In this study, the recovery of nitrate reduction activity or even preferential reduction cannot be explained from the perspective of electron transport and consumption. Therefore, a question was waiting to be answered: why nitrate reduction was not affected when NAR activity, like NIR activity, was inhibited?

3.3. Abundance and expression of denitrifying functional genes

In addition to denitrifying enzyme activity, the reduction of nitrogen species also depends on the corresponding genetic regulation (Hassan et al., 2016). In this study, the effects of low temperature on the abundance and expression of core denitrification genes, *narG*, *nirS*, *nirK*, and *nosZ*, were evaluated. The *nosZ* gene was used to indicate the potential function of microbial community to reduce N₂O and to predict the emission potential of N₂O (Orellana et al., 2014). As shown in Fig. 4a, the copy numbers of the *narG* and *nirK* genes decreased slightly after prolonged exposure to low temperature. Moreover, the *nirS* gene copy numbers declined significantly by more than two orders of magnitude, from 2.09×10^9 to 6.74×10^6 copies/g VSS. The change in *nosZ* gene abundance also showed a similar tendency, with the average copies decreasing from 3.31×10^8 to 1.11×10^7 copies/g VSS. These results showed that the abundance of all tested genes was higher in the control compared with T15 treatment, suggesting that HPHD system has a stronger potential denitrification capability at 30 °C.

The genes *nirS* and *nirK* are the most common genetic markers for characterizing the dynamic shift of denitrifying communities (Philippot and Hallin, 2005; Wallenstein et al., 2006). Previous studies pointed out that the distinct temperature differences may influence the population dynamics of denitrifier communities, thus affecting intermediate accumulation and denitrification activity (Chon et al., 2011; Liao et al., 2018). In this study, the abundance of *nirS*-gene-bearing denitrifiers at 30 °C was much higher than *nirK*-gene-bearing denitrifiers. With the temperature dropped to 15 °C, the population of *nirS*-gene-bearing denitrifiers no longer showed a significant dominance compared to those bearing *nirK* gene. The strong variation in community composition suggested that different denitrifying bacteria were active at different temperatures, whereas *nirS*-gene-bearing denitrifiers were more sensitive to psychrophilic temperature. In addition, the substantial accumulation of nitrite in T15 treatment may be related to the sharp decrease in *nirS* gene abundance because of the potential correlation between the *nirS* gene encoding NIR and nitrite reduction activity.

The fluctuation of functional gene abundance in the environment does not necessarily imply that the corresponding bacteria will present

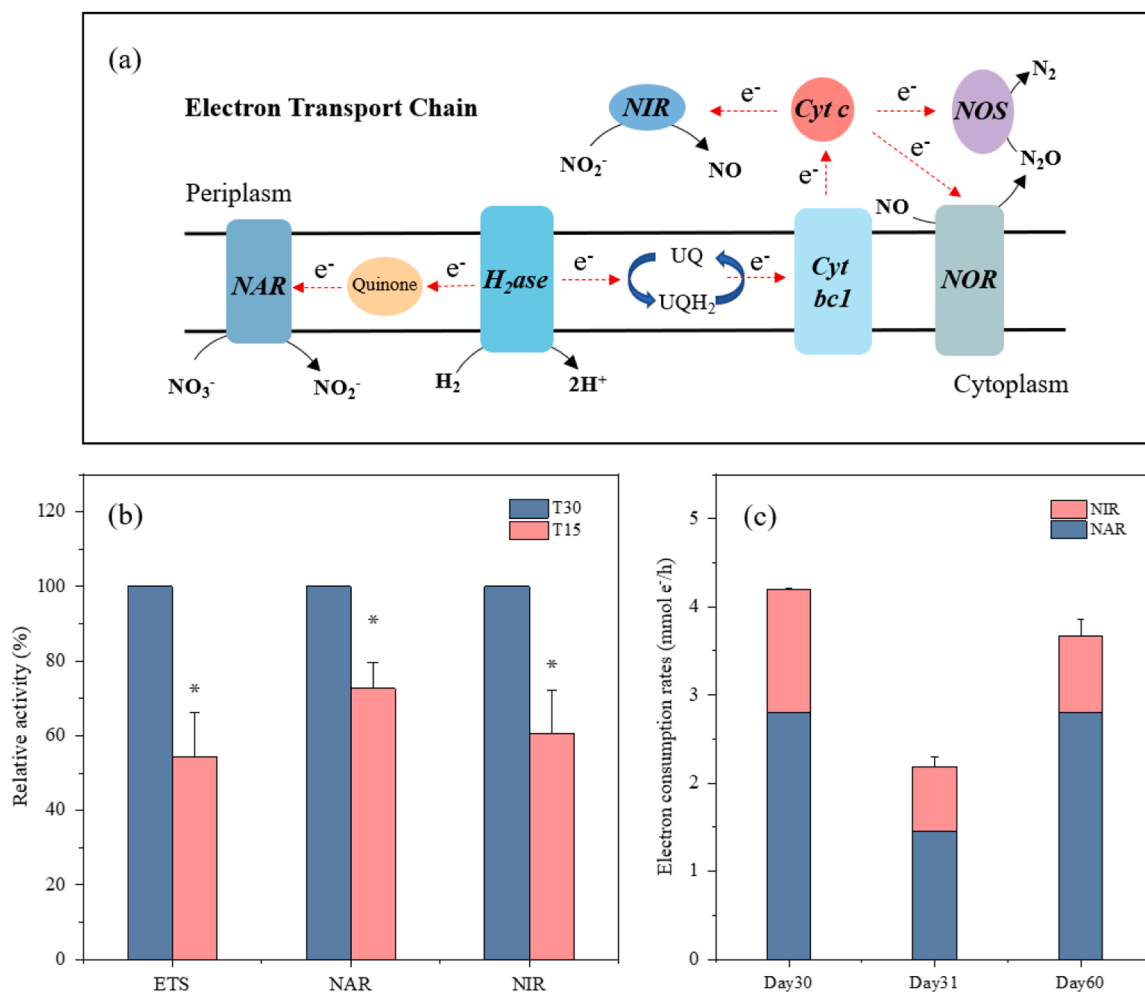


Fig. 3. Schematic diagram of canonical electron transport chain in hydrogenotrophic denitrification (a), and effects of temperature variation on ETS and denitrifying enzyme activities (b). Error bars represent the standard deviations of six independent tests ($n = 6$). Asterisks (*) indicate significant differences with the control (independent samples t -test, $p < 0.05$). Electron consumption rates by NAR and NIR, with error bars representing standard deviations associated with the total consumption rates (c). NAR: nitrate reductase, NIR: nitrite reductase, NOR: nitric oxide reductase, NOS: nitrous oxide reductase, H_2ase : hydrogenase, Cyt: cytochrome.

the expected dynamics of denitrification activity (Chen and Vymazal, 2015; Philippot and Hallin, 2005). Therefore, the relative expression of functional genes was quantified to allow a more accurate reflection of the actual denitrification activity. As shown in Fig. 4b, compared with the control, the expression of the *narG* gene was significantly up-regulated by $54.7 \pm 5.86\%$ after long-term incubation at 15°C ($p < 0.05$). This is a reasonable explanation for the fact that the decrease in temperature did not inhibit the nitrate reduction. Meanwhile, the expression of the *nirS* gene was significantly down-regulated by $73.7 \pm 5.13\%$ due to decreased temperature ($p < 0.05$), while temperature dependency of the *nirK* gene expression was not observed. Saleh-Lakha et al. showed that the delayed induction and expression of the *nirS* gene in pure cultures of *Pseudomonas mandelii* as the temperature decreased led to a lag in NIR synthesis, which was responsible for nitrite accumulation during denitrification (Saleh-Lakha et al., 2009). This further corroborated that the potential nitrite production was more active than its reduction in T15 treatment. Furthermore, the *nosZ* gene expression was much higher than that of the control, which was significantly up-regulated by $108.3 \pm 11.2\%$ ($p < 0.05$). It was reported that the *nosZ* gene expression level rather than gene abundance regulated N_2O emission (Su et al., 2019). Therefore, it could predict reasonably that extra N_2O emissions may not be induced when HPHD system operates under low temperatures.

Comprehensive consideration of the abundance and structure of

microflora and their actual activity in specific environments may contribute to shed light on the cause of the mismatch between nitrogen transformation and functional gene abundance. (Chen et al., 2015; Philippot and Hallin, 2005). Prolonged exposure to cold condition altered the abundance of functional genes in the denitrifying community and the *narG* gene abundance declined, but NO_3^- -N reduction rates were maintained at a high level. In contrast, NO_2^- -N reduction was greatly inhibited in the presence of a significant decrease in the abundance of the genes encoding NIR (*nirS* and *nirK* genes). In fact, denitrification enzymes (enzyme synthesis and activity) are the direct factors that govern nitrogen transformation in terms of single enzymatic steps (Zumft, 1997). The effects of temperature on the induction levels and timings of various denitrifying functional genes were significantly different (Saleh-Lakha et al., 2009). Therefore, the discrepancy between the reduction of nitrate and nitrite in response to low temperature is mainly attributable to the significant up-regulation of *narG* gene expression for NAR production and the significant down-regulation of *nirS* gene expression for NIR production. This study revealed that the regulation of gene expression may be more significant than gene abundance in determining nitrogen species transformation, which suggested that it might be possible to eliminate intermediates accumulation or promote intermediates recovery during denitrification by regulating the physiological activity of denitrifiers via exerting selective pressure.

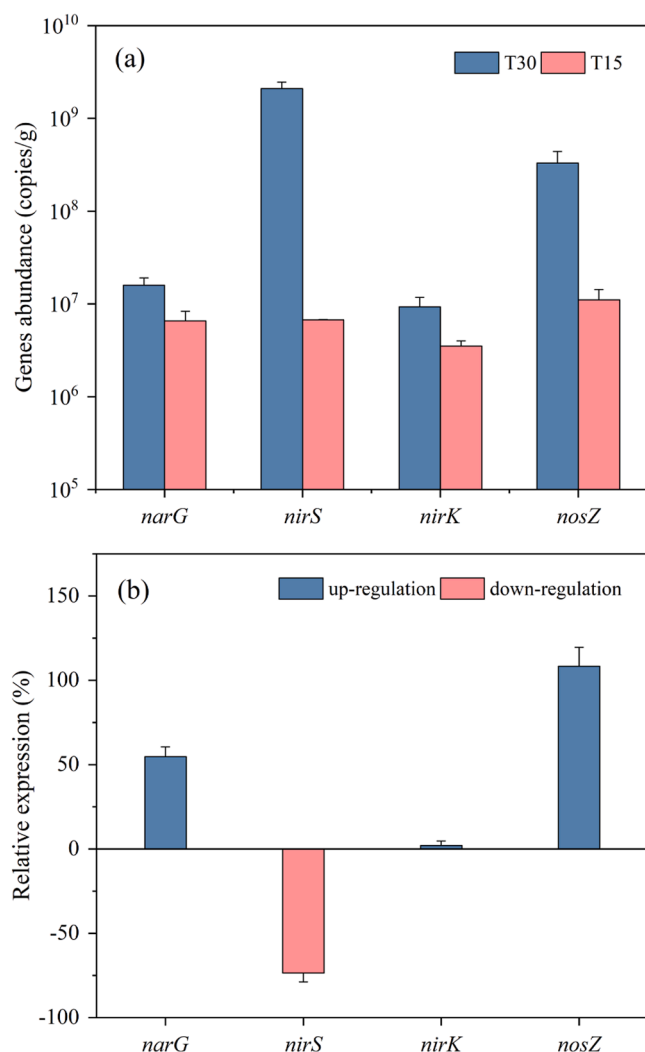


Fig. 4. Effects of low temperature on the copy number (a), and relative expression (b) of denitrifying functional genes, *narG*, *nirS*, *nirK*, and *nosZ*. Error bars represent standard deviations of three replicates.

3.4. Shift of bacterial community in hydrogenotrophic denitrifying culture

Bacterial community composition of hydrogenotrophic denitrification at different temperatures was analyzed based on 16S rRNA high-throughput sequencing, and the phylogenetic classification was characterized at the phylum and genus levels (Fig. 5). Metrics for assessing community richness and diversity, such as richness estimators (Chao and observed species) and diversity indices (Shannon and Simpson), were listed in Table S3. At the phylum level, *Proteobacteria* dominated in both phases, accounting for more than 90 % of the bacterial community, followed by *Bacteroidetes*. Previous reports have also shown that *Proteobacteria* was the most abundant phyla of the microbial community in the hydrogenotrophic reactor (Li et al., 2017; Xiao et al., 2015). *Paracoccus* belonging to the α -*Proteobacteria* and *Hydrogenophaga*, members of the β -*Proteobacteria*, were the main potential denitrifier genera detected. In addition, there were four genera (*Flavobacterium*, *Thauera*, *Chryseobacterium*, *Stappia*) that account for more than 1 % in phase I or phase II. The relative abundances of *Paracoccus* and *Hydrogenophaga* genera varied greatly at different temperatures, suggesting that the microbial community structure of hydrogenotrophic denitrification was significantly altered. Specifically, the relative abundance of *Paracoccus* was much higher at 30 °C but decreased from 73.9 % to 37.6 % at the end of phase II, while the relative abundance of *Hydrogenophaga*

increased gradually from 12.9 % to 48.2 % at 15 °C, replacing *Paracoccus* as the dominant genus.

In general, most *Paracoccus* species were considered as versatile microorganisms with mixotrophic metabolism (Baker et al., 1998), however, they were less competitive at low temperatures. Nitrite accumulation was not observed in a hydrogenotrophic denitrification kinetics study on pure cultures of *Paracoccus.sp* (Vasiliadou et al., 2006). In addition, the high nitrite accumulation at 15 °C in this study may be related to the enrichment of *Hydrogenophaga* in phase II. The genus *Hydrogenophaga* has been reported as an important group for nitrate removal and nitrite production that plays a significant role in partial hydrogenotrophic denitrification (Shinoda et al., 2020). It is attributed to the unique denitrification regulatory phenotype of *Hydrogenophaga* species, i.e., the progressive onset of denitrification reactions. While available, electrons from H₂ oxidation only flowed to NAR until nitrate was depleted and then to NIR in *Hydrogenophaga taeniospiralis* (Duffner et al., 2022).

In conclusion, hydrogenotrophic denitrifiers involved limited genera, and the microbial community had a low diversity in hydrogenotrophic denitrification. This is due to the highly selective nature of the H₂-driven denitrifying environment (Karanasios et al., 2010). However, it should be noted that simulating in situ wastewater treatment under laboratory conditions has inherent limitations in the enrichment of functional microorganisms owing to the single function performed. In addition, it was postulated that the accumulation of denitrification intermediates resulted from electron competition among various nitrogen oxide reductases (Pan et al., 2013). However, our results preferred that this might be the result of competition between denitrifying bacteria with different denitrification phenotypes in the microbial community. This finding provides a new insight in revealing the impacts of community succession on the performance of hydrogenotrophic denitrification systems.

4. Conclusion

In this study, the nitrate reduction gradually recovered after acclimation while high nitrite accumulated in HPHD. When the temperature dropped from 30 °C to 15 °C, the SDR decreased from 38.9 ± 1.5 to 24.4 ± 2.3 mg N/(gVSS·h), accompanied by nitrite accumulation up to 40.3 ± 3.0 mg/L. The negative effect of low temperature shock on ETS and denitrifying enzyme activities was directly responsible for the significant SDR decline. The *narG* gene expression significantly increased by 54.7 % while the *nirS* gene expression decreased by 73.7 % at 15 °C, which was the primary cause of high nitrite accumulation under long-term low temperature stress. Moreover, the microbial community structure of hydrogenotrophic culture was altered, with the dominant populations shifting from the genera *Paracoccus* to *Hydrogenophaga*, and as a result, the population of *nirS*-gene-bearing denitrifiers declined greatly.

CRedit authorship contribution statement

Jianmin Zhou: Writing – original draft, Visualization, Investigation, Formal analysis, Data curation, Conceptualization. **Lei Ding:** Writing – review & editing, Supervision, Funding acquisition, Conceptualization. **Changzheng Cui:** Writing – review & editing. **Ralph E.F. Lindeboom:** Writing – review & editing.

Declaration of competing interest

The authors declare that they have no known competing financial interests or personal relationships that could have appeared to influence the work reported in this paper.

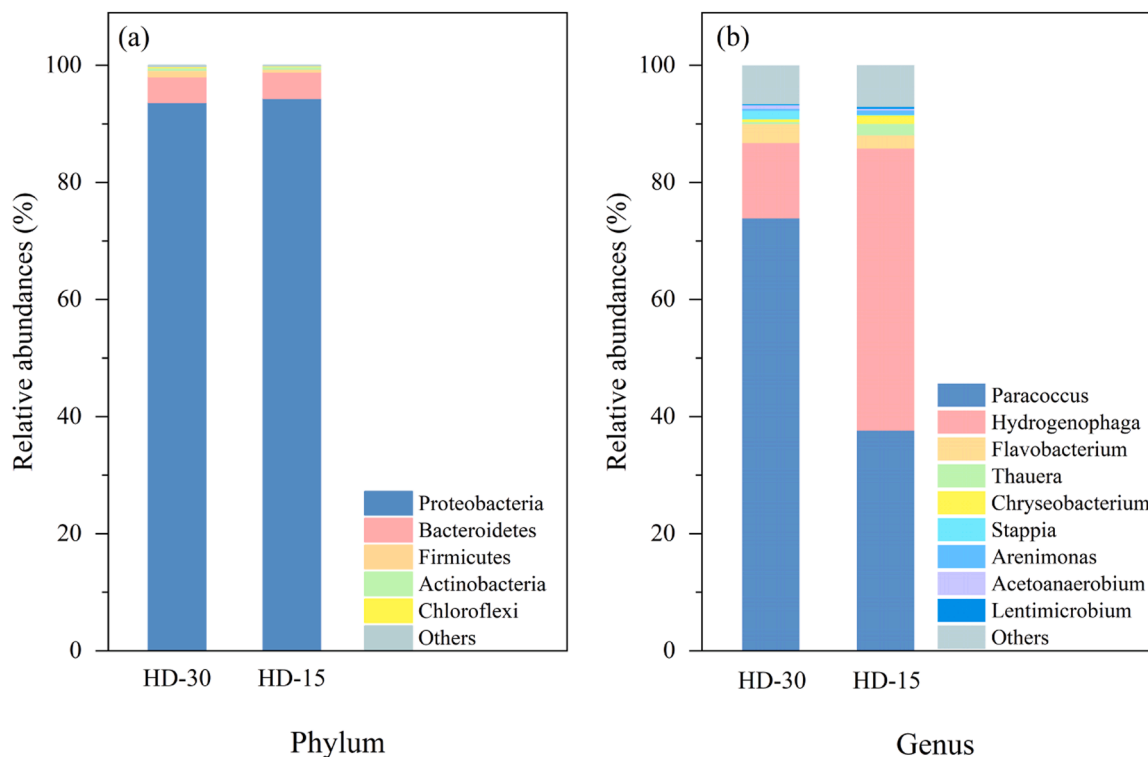


Fig. 5. Bacterial community composition at the phylum level (a) and the genus level (b) based on taxonomic assignment of 16S rRNA gene sequences (HD-30, 30 °C; HD-15, 15 °C. Sequence percentage > 0.1 %).

Data availability

Data will be made available on request.

Acknowledgements

This work was supported by the Scientific Research Foundation for the Returned Overseas Chinese Scholars, State Education Ministry (B100-C-1503), and the National Natural Science Foundation of China (51008125).

Supplementary materials

Supplementary material associated with this article can be found, in the online version, at [doi:10.1016/j.watres.2024.122144](https://doi.org/10.1016/j.watres.2024.122144).

References

- Albina, P., Durban, N., Bertron, A., Albrecht, A., Robinet, J.C., Erable, B., 2019. Influence of hydrogen electron donor, alkaline pH, and high nitrate concentrations on microbial denitrification: a review. *Int. J. Mol. Sci.* 20 (20), 5163.
- Almeida, J., Reis, M., Carrondo, M., 1995. Competition between nitrate and nitrite reduction in denitrification by *Pseudomonas fluorescens*. *Biotechnol. Bioeng.* 46 (5), 476–484.
- APHA, 2005. *Standard Methods for the Examination of Water and Wastewater*. American Water Works Association and Water Environment Federation, 21st ed. American Public Health Association, Washington, DC, USA.
- Baker, S.C., Ferguson, S.J., Ludwig, B., Page, M.D., Richter, O.M.H., van Spanning, R.J., 1998. Molecular genetics of the genus *Paracoccus*: metabolically versatile bacteria with bioenergetic flexibility. *Microbiol. Mol. Biol. Rev.* 62 (4), 1046–1078.
- Bolyen, E., Rideout, J.R., Dillon, M.R., Bokulich, N.A., Abnet, C., Al-Ghalith, G.A., Alexander, H., Alm, E.J., Arumugam, M., Asnicar, F., 2018. QIIME 2: reproducible, interactive, scalable, and extensible microbiome data science. *PeerJ Prepr.* 6, e27295v2.
- Bowien, B., Schlegel, H.G., 1981. Physiology and biochemistry of aerobic hydrogen-oxidizing bacteria. *Annu. Rev. Microbiol.* 35 (1), 405–452.
- Broberg, A., 1985. A modified method for studies of electron transport system activity in freshwater sediments. *Hydrobiologia* 120 (2), 181–187.
- Canfield, D.E., Glazer, A.N., Falkowski, P.G., 2010. The evolution and future of Earth's nitrogen cycle. *Science* 330 (6001), 192–196.
- Chen, L.P., Huang, F.Y., Zhang, C., Zhang, J., Liu, F., Guan, X.Y., 2021. Effects of norfloxacin on nitrate reduction and dynamic denitrifying enzymes activities in groundwater. *Environ. Pollut.* 273, 116492.
- Chen, Y., Vymazal, J., 2015. Comment on “enhanced long-term nitrogen removal and its quantitative molecular mechanism in tidal flow constructed wetlands. *Environ. Sci. Technol.* 49 (18), 11241–11242.
- Chen, Y.W., Lan, S.H., Wang, L.H., Dong, S.Y., Zhou, H.Z., Tan, Z.L., Li, X.D., 2017. A review: driving factors and regulation strategies of microbial community structure and dynamics in wastewater treatment systems. *Chemosphere* 174, 173–182.
- Chen, Z., Wang, C.H., Gschwendtner, S., Willibald, G., Unteregelsbacher, S., Lu, H.Y., Kolar, A., Schloter, M., Butterbach-Bahl, K., Dannenmann, M., 2015. Relationships between denitrification gene expression, dissimilatory nitrate reduction to ammonium and nitrous oxide and dinitrogen production in montane grassland soils. *Soil Biol. Biochem.* 87, 67–77.
- Chon, K., Chang, J.S., Lee, E., Lee, J., Ryu, J., Cho, J., 2011. Abundance of denitrifying genes coding for nitrate (*narG*), nitrite (*nirS*), and nitrous oxide (*nosZ*) reductases in estuarine versus wastewater effluent-fed constructed wetlands. *Ecol. Eng.* 37 (1), 64–69.
- Di Capua, F., Milone, I., Lakanieni, A.M., Lens, P.N.L., Esposito, G., 2017. High-rate autotrophic denitrification in a fluidized-bed reactor at psychrophilic temperatures. *Chem. Eng. J.* 313, 591–598.
- Duffner, C., Kublik, S., Fasel, B., Frostegard, A., Schloter, M., Bakken, L., Schulz, S., 2022. Genotypic and phenotypic characterization of hydrogenotrophic denitrifiers. *Environ. Microbiol.* 24 (4), 1887–1901.
- Epsztein, R., Beliaevski, M., Tarre, S., Green, M., 2016. High-rate hydrogenotrophic denitrification in a pressurized reactor. *Chem. Eng. J.* 286, 578–584.
- Epsztein, R., Desitti, C., Beliaevski, M., Tarre, S., Green, M., 2017. Co-reduction of nitrate and perchlorate in a pressurized hydrogenotrophic reactor with complete H₂ utilization. *Chem. Eng. J.* 328, 133–140.
- Hassan, J., Qu, Z., Bergaust, L.L., Bakken, L.R., 2016. Transient accumulation of NO₂ and N₂O during denitrification explained by assuming cell diversification by stochastic transcription of denitrification genes. *PLoS Comput. Biol.* 12 (1), e1004621.
- Karanasios, K.A., Vasiladiou, I.A., Pavlou, S., Vayenas, D.V., 2010. Hydrogenotrophic denitrification of potable water: a review. *J. Hazard. Mater.* 180 (1–3), 20–37.
- Keisar, I., Desitti, C., Beliaevski, M., Epsztein, R., Tarre, S., Green, M., 2021. A pressurized hydrogenotrophic denitrification reactor system for removal of nitrates at high concentrations. *J. Water Process Eng.* 42, 102140.
- Knowles, C.J., 1980. *Diversity of Bacterial Respiratory Systems*. CRC Press, Boca Raton, FL.
- Kuypers, M.M.M., Marchant, H.K., Kartal, B., 2018. The microbial nitrogen-cycling network. *Nat. Rev. Microbiol.* 16 (5), 263–276.

- Lee, K.C., Rittmann, B.E., 2002. Applying a novel autohydrogenotrophic hollow-fiber membrane biofilm reactor for denitrification of drinking water. *Water Res.* 36 (8), 2040–2052.
- Li, P., Wang, Y., Zuo, J., Wang, R., Zhao, J., Du, Y., 2017. Nitrogen removal and N₂O accumulation during hydrogenotrophic denitrification: influence of environmental factors and microbial community characteristics. *Environ. Sci. Technol.* 51 (2), 870–879.
- Li, P., Xing, W., Zuo, J., Tang, L., Wang, Y., Lin, J., 2013. Hydrogenotrophic denitrification for tertiary nitrogen removal from municipal wastewater using membrane diffusion packed-bed bioreactor. *Bioresour. Technol.* 144, 452–459.
- Liao, R., Miao, Y., Li, J., Li, Y., Wang, Z., Du, J., Li, Y., Li, A., Shen, H., 2018. Temperature dependence of denitrification microbial communities and functional genes in an expanded granular sludge bed reactor treating nitrate-rich wastewater. *RSC Adv.* 8 (73), 42087–42094.
- Livak, K.J., Schmittgen, T.D., 2001. Analysis of relative gene expression data using real-time quantitative PCR and the $2^{-\Delta\Delta CT}$ method. *Methods* 25 (4), 402–408.
- Orellana, L.H., Rodriguez-R, L.M., Higgins, S., Chee-Sanford, J.C., Sanford, R.A., Ritalahti, K.M., Löffler, F.E., Konstantinidis, K.T., 2014. Detecting nitrous oxide reductase (*nosZ*) genes in soil metagenomes: method development and implications for the nitrogen cycle. *MBio* 5 (3), 10.1128.
- Pan, Y.T., Ni, B.J., Bond, P.L., Ye, L., Yuan, Z.G., 2013. Electron competition among nitrogen oxides reduction during methanol-utilizing denitrification in wastewater treatment. *Water Res.* 47 (10), 3273–3281.
- Philippot, L., Hallin, S., 2005. Finding the missing link between diversity and activity using denitrifying bacteria as a model functional community. *Curr. Opin. Microbiol.* 8 (3), 234–239.
- Ren, Z.J., Pagilla, K., 2022. Pathways to Water Sector Decarbonization, Carbon Capture and Utilization. IWA Publishing.
- Rezania, B., Oleszkiewicz, J.A., Cicek, N., 2007. Hydrogen-dependent denitrification of water in an anaerobic submerged membrane bioreactor coupled with a novel hydrogen delivery system. *Water Res.* 41 (5), 1074–1080.
- Rittmann, B.E., 2018. Biofilms, active substrata, and me. *Water Res.* 132, 135–145.
- Saleh-Lakha, S., Shannon, K.E., Henderson, S.L., Goyer, C., Trevors, J.T., Zebarth, B.J., Burton, D.L., 2009. Effect of pH and temperature on denitrification gene expression and activity in *Pseudomonas mandelii*. *Appl. Environ. Microbiol.* 75 (12), 3903–3911.
- Shen, Q.S., Ji, F.Y., Wei, J.Z., Fang, D.X., Zhang, Q., Jiang, L., Cai, A.R., Kuang, L., 2020. The influence mechanism of temperature on solid phase denitrification based on denitrification performance, carbon balance, and microbial analysis. *Sci. Total Environ.* 732, 139333.
- Shinoda, K., Eamrat, R., Tsutsumi, Y., Rujakom, S., Singhon, T., Kamei, T., Kazama, F., 2020. Newly established process combining partial hydrogenotrophic denitrification and anammox for nitrogen removal. *Water Sci. Technol.* 82 (7), 1272–1284.
- Su, X., Chen, Y., Wang, Y., Yang, X., He, Q., 2019. Impacts of chlorothalonil on denitrification and N₂O emission in riparian sediments: microbial metabolism mechanism. *Water Res.* 148, 188–197.
- Tang, Y.N., Zhou, C., Ziv-El, M., Rittmann, B.E., 2011. A pH-control model for heterotrophic and hydrogen-based autotrophic denitrification. *Water Res.* 45 (1), 232–240.
- Tian, T., Yu, H.Q., 2020. Denitrification with non-organic electron donor for treating low C/N ratio wastewaters. *Bioresour. Technol.* 299, 122686.
- Vasiliadou, I.A., Siozios, S., Papadas, I.T., Bourtzis, K., Pavlou, S., Vayenas, D.V., 2006. Kinetics of pure cultures of hydrogen-oxidizing denitrifying bacteria and modeling of the interactions among them in mixed cultures. *Biotechnol. Bioeng.* 95 (3), 513–525.
- Wallenstein, M.D., Myrold, D.D., Firestone, M., Voytek, M., 2006. Environmental controls on denitrifying communities and denitrification rates: insights from molecular methods. *Ecol. Appl.* 16 (6), 2143–2152.
- Wan, R., Chen, Y.G., Zheng, X., Su, Y.L., Li, M., 2016. Effect of CO₂ on microbial denitrification via inhibiting electron transport and consumption. *Environ. Sci. Technol.* 50 (18), 9915–9922.
- Wang, S.K., Wang, Y.J., Li, P., Wang, L., Su, Q.X., Zuo, J.N., 2022. Development and characterizations of hydrogenotrophic denitrification granular process: nitrogen removal capacity and adaptability. *Bioresour. Technol.* 363, 127973.
- Wang, X.J., Ye, C.S., Zhang, Z.J., Guo, Y., Yang, R.L., Chen, S.H., 2018. Effects of temperature shock on N₂O emissions from denitrifying activated sludge and associated active bacteria. *Bioresour. Technol.* 249, 605–611.
- Xiao, Y., Zheng, Y., Wu, S., Yang, Z.H., Zhao, F., 2015. Bacterial community structure of autotrophic denitrification biocathode by 454 pyrosequencing of the 16S rRNA gene. *Microb. Ecol.* 69 (3), 492–499.
- Zhou, J., Ding, L., Shi, M., Lindeboom, R.E., Cui, C., 2022. The key factor in high pressure hydrogenotrophic denitrification: hydrogen partial pressure. *J. Water Process. Eng.* 49, 103195.
- Zumft, W.G., 1997. Cell biology and molecular basis of denitrification. *Microbiol. Mol. Biol. Rev.* 61 (4), 533–616.